PERMAFROST AND PERIGLACIAL PROCESSES
Permafrost Periglac. Process. **14**: 125–139 (2003)
Published online in Wiley InterScience (www.interscience.wiley.com). DOI: 10.1002/ppp.449

A Model for Regional-Scale Estimation of Temporal and Spatial Variability of Active Layer Thickness and Mean Annual Ground Temperatures

*T. S. Sazonova and V. E. Romanovsky**

Geophysical Institute, University of Alaska-Fairbanks, USA

ABSTRACT

High-latitude ecosystems where the mean annual ground surface temperature is around or below 0 °C are highly sensitive to global warming. This is largely because these regions contain vast areas of permafrost, which begins to thaw when the mean annual temperature rises above freezing. The Geophysical Institute Permafrost Lab has developed a new interactive geographical information systems (GIS) model to estimate the long-term response of permafrost to changes in climate. An analytical approach is used for calculating both active layer thickness (ALT) and mean annual ground temperatures (MAGTs). When applied to long-term (decadal or longer time scale) averages, this approach shows an accuracy of ±0.2–0.4 °C for MAGTs and ±0.1–0.3 m for ALT calculations. The relative errors do not exceed 32% for ALT calculations, but typically they are between 10 and 25%. A spatial statistical analysis of the data from 32 sites in Siberia indicated a confidence level of 75% to have a deviation between measured and calculated MAGTs of 0.2–0.4 °C. A detailed analysis has been performed for two regional transects in Alaska and eastern Siberia that has validated the use of the model. The results obtained from this analysis show that a more economical (in terms of computational time) analytical approach could be successfully used instead of a full-scale numerical model in the regional and global scale analysis of permafrost spatial and temporal dynamics. This project has been a successful contribution to the Arctic Climate Impact Assessment project. Copyright © 2003 John Wiley & Sons, Ltd.

KEY WORDS: active layer; ground temperatures; permafrost; modelling; GIS

INTRODUCTION

There is an immediate need to evaluate climate dynamics and the respective impact on high-latitude ecosystems. The effects of global climate change are expected to be amplified in the Arctic, where a slight increase in mean annual air temperature can result in a change of state for large regions of frozen ground (Kattenberg *et al.*, 1996; Anisimov *et al.*, 2001).

Permafrost regions occupy about one quarter of land surface of the northern hemisphere (Péwé, 1983; Zhang *et al.*, 2000). The changing properties of permafrost play an important role in driving the ecosystem balance, and affecting the carbon and water cycles. Man-made structures built on or near ice-rich permafrost have been known to be severely damaged by thaw-induced settling of the ground, which will accelerate if mean annual temperatures continue to rise (Osterkamp *et al.*, 1997; Smith and Burgess, 1999). The carbon and water cycles can be dramatically affected by an increased thickness of the active layer which thaws seasonally.

* Correspondence to: Dr. V. E. Romanovsky, Geophysical Institute, University of Alaska-Fairbanks, PO Box 757320, Fairbanks, Alaska 99775-7320, USA. E-mail: ffver@uaf.edu

Received 15 January 2003
Revised 30 March 2003
Accepted 4 April 2003

Copyright © 2003 John Wiley & Sons, Ltd.

The purpose of this research was to develop a model which can be used to evaluate active layer thickness (ALT) and mean annual ground temperatures (MAGTs) over large regions (such as the east Siberian and Alaskan transects of International Geosphere-Biosphere Program). Sufficient accuracy and spatial resolution are required so that it can be applied effectively to current climatological and ecological models. Our model, the Geophysical Institute Permafrost Lab (GIPL) model was designed specifically to assess the effect of a changing climate on permafrost. The results have been used in the Arctic Climate Impact Assessment (ACIA) program (www.acia.uaf.edu), which was designed to investigate the various impacts of future climate change on timescales of up to 100 years.

A transect approach is considered to be the most effective method for modelling permafrost dynamics because of problems with collecting data over large high-latitude regions. This method analyses permafrost dynamics along several latitudinal transects where different types of environmental conditions exist. After analysis of these transects is complete, they can be used to interpolate the permafrost dynamics over other temporal and spatial domains leading eventually to circum-polar coverage.

The two areas we have analysed differ significantly in the information available on climate, vegetation, and soil properties (Figure 1). Despite these differences, previous investigations and point by point comparisons of different sites have shown that variations in ground temperatures within the transects are consistent (Shender *et al.*, 1999; Romanovsky *et al.*, 2001). The climatic parameters we used to evaluate permafrost dynamics in the future were provided by the ACIA program and were output from six global climate models (GCMs).

A number of algorithms have been developed to determine ALT and permafrost distribution. One such approach, based on Kudryavtsev's method, was developed to provide a spatially distributed analytical model that estimates the maximum annual thaw depth (ALT). In this approach, geographical information systems (GIS) were used to incorporate climate records, field data and digital mapping techniques to estimate ALT (Shiklomanov and Nelson, 1999). This analysis was applied over a 22 300 km^2 area in the Kuparuk River basin, north-central Alaska.

The introduction of GCMs made it possible to evaluate permafrost dynamics on a global scale. Anisimov and Nelson (1997) used a frost index approach (Nelson and Outcalt, 1987), coupled with three GCMs to develop the first GCM-based assessment of permafrost dynamics over the northern hemisphere. The results indicated that a large, nearly circum-polar zone of relict permafrost would develop by the end of the 21st century.

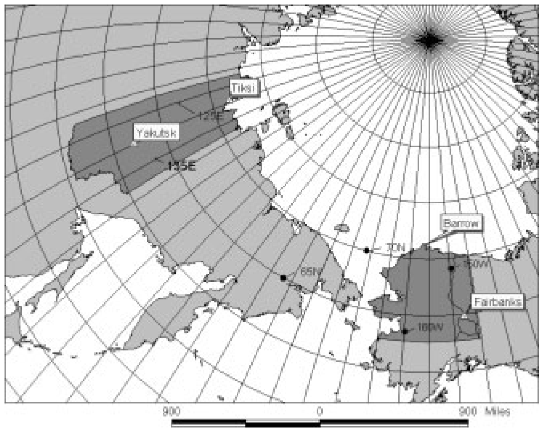

Figure 1 East Siberian Tiksi–Yakutsk and Alaskan Barrow–Fairbanks transects.

The most recent application of GCMs to determine permafrost dynamics has been done by Stendel and Christensen (2002). They calculated ALT using the modified Stefan's equation. The results of this work indicated that ALT will increase by 30–40% by the end of the 21st century.

The models developed by Anisimov and Nelson (1997), and Stendel and Christensen (2002) have a spatial resolution of about 2.5–5° latitude/longitude. This resolution does not allow for complex relief and vegetation patterns, and is a rough approximation for applications in ecosystem modelling and infrastructure risk assessment. For the purposes of this project, it was determined that a spatial resolution of $0.5 \times 0.5°$ would be appropriate for modelling on a regional scale. It should be mentioned that the authors never aimed at creating a highly accurate model, which is not feasible with a resolution scale of $0.5 \times 0.5°$ latitude/longitude. It was most important to create a physically-based model which well describes the temporal-dynamic aspects.

GIPL allows for the calculation of ALT and MAGTs at the bottom of the active layer. For areas with permafrost, this temperature is the same as mean annual temperature at the permafrost table. Where permafrost is absent, MAGT is the mean annual temperature at the bottom of the seasonally frozen layer. The MAGT is important because it reflects the existence and thermal stability of the permafrost. When MAGT becomes positive (above 0 °C), the winter freezing front does not reach the surface of permafrost (permafrost table) by the end of cold

Copyright © 2003 John Wiley & Sons, Ltd.

season, resulting in talik formation and the start of permafrost degradation. Permafrost degradation could also start when MAGT is still below 0 °C. If the increasing ALT reaches the ice horizon, or the ground layer with high ice content, the ice begins to melt and the ground subsides. Surface water will flow into the deepening trough and can form pools and lakes. This new presence of water on the surface will help thermal energy to penetrate the ground faster, resulting in an acceleration of permafrost degradation. In winter, more snow will settle into the deepening trough, which will additionally insulate the ground, resulting in an increased MAGT. This will prevent the winter freeze from penetrating to the permafrost table, further accelerating degradation (Kudryavtsev *et al*., 1974; Yershov, 1998). Because of these effects, once permafrost begins to thaw and a significant settlement of the ground surface has occurred, the process would continue even through colder winters, which would otherwise be expected to resist the degradation process.

The GIPL model focuses on calculation of ALT and MAGT, but does not calculate the depth of permafrost thawing from the surface. Other models need to be used to calculate the timing and dynamics of permafrost degradation (Kudryavtsev *et al*., 1974; Kane *et al*., 1991; Hinzman *et al*., 1997). The cross of this temperature threshold will have a crucial effect on northern ecosystems through changes in thermal and hydrological conditions in soils, and can effect changes in the carbon cycle on a global scale.

This paper describes the basic concept and structure of the GIPL model. The calibration of the model and evaluation of the model's performance will be discussed to assess possible uncertainties associated with data handling and processing.

DESCRIPTION OF THE GIPL MODEL

The GIPL model consists of two parts. The GIS approach allows visual analysis of the spatial distribution of various geographical parameters. With this approach, the results from analytical or numerical models can be applied to evaluate permafrost parameters over large geographic areas. The second part of the model is an analytical solution which is used for the evaluation of major permafrost properties, such as MAGT and ALT.

Throughout the years, simplified analytical solutions for ALT have been applied for structural engineering and other practical purposes. Most of these methods have been based on the Stefan solutions, and they do not yield a good level of accuracy (Romanovsky and Osterkamp, 1997). Two factors played the primary role in choosing a method for calculating ALT: the model should be relatively simple and have a reasonable computation time, and must have an acceptable degree of accuracy. It was determined that the best method for computation of ALT and MAGTs was a modified Kudryavtsev's approach (mKA) (Romanovsky and Osterkamp, 1997). The mKA approach is the core of the GIPL model.

In their work on ALT distribution, Shiklomanov and Nelson (1999) and Anisimov and Nelson (1997) demonstrated that Kudryavtsev's approach works well. The research showed that the approach allows for consideration of variations in conditions such as snow cover and vegetation (Shiklomanov and Nelson, 1999). This approach had several shortcomings due to factors such as neglect of unfrozen water, and treating the ground as being homogeneous. Still, the method was shown to allow estimation of permafrost temperatures to within 0.5 °C.

mKA

Kudryavtsev's approach was chosen because it effectively accounts for the effects of snow cover, vegetation, soil moisture, thermal properties, and regional climate variations. The approach was developed to find MAGTs and ALT while taking into account major geological and geographical factors and assuming a periodical, quasi-steady-state temperature regime (Kudryavtsev *et al*., 1974).

The daylight surface (ground or vegetation surface during the summer and snow surface during the winter) temperature is assumed to behave in accordance with:

$$T(t) = T_a + A_a \sin\left(\frac{2\pi}{\tau}t\right)$$

where A_a is the seasonal amplitude of air temperatures °C, T_a is the mean annual air temperature, τ is the period which is equivalent to one year, and t is time. The ground is assumed to have homogeneous thermal conductivity. The effects of geothermal heat flux are ignored because it is considered to have a minimal contribution to MAGT and ALT values.

Kudryavtsev introduced the idea of applying the Fourier temperature wave propagation theory on a medium with phase transitions, such as frozen ground (Tikhonov and Samarsky, 1966). Application of this approach resulted in the discovery of the thermal offset and an understanding of the laws that govern the dynamics of the ground thermal regime. These discoveries led to an understanding of the effects

Copyright © 2003 John Wiley & Sons, Ltd.

that thermophysical properties of the ground have on MAGTs and ALT, and how periodically varying climatic parameters affect permafrost dynamics. The output parameters of this method are given as annual averages. Input and output parameters are listed in Tables 1 and 2.

Kudryavtsevs's approach treats the complex system considering air, snow cover, surface vegetation, and active layer, as a set of individual layers with different thermal properties. In the regions of Alaska and east Siberia that were analysed, surface vegetation consists of lichens, grass, and moss (sphagnum or feather mosses) (Feldman *et al.*, 1988; Brown and Kreig, 1983). The upper level of vegetation consists of trees and shrubs (vegetation taller than 50 cm) and was not considered in the computation. This upper level vegetation affects the thickness and density of the snow cover, along with the amount of solar radiation which is incident on the ground surface. In our study we considered only low-level vegetation (surface vegetation) less than 0.5 m high, because information about higher vegetation such as trees and tall shrubs is already incorporated into the monthly surface air temperature data, which were used as input data in the model. Also, effective methods for calculating the thermal effects of vegetation are still under development (Potter *et al.*, 2001; Friend *et al.*, 1997).

Table 1 Input variables and parameters.

Input variables	Notation	Units
Seasonal range of air temperature variations	A_a	°C
Mean annual air temperature	T_a	°C
Winter-averaged snow thickness	H_{sn}	m
Snow density	ρ_{sn}	kg/m^3
Thermal conductivity of snow	K_{sn}	W/(m*K)
Height of vegetation cover	H_v	m
Thermal diffusivity of vegetation in frozen state	D_{vf}	m^2/s
Thermal diffusivity of vegetation in thawed state	D_{vt}	m^2/s
Thermal conductivity of frozen ground	K_f	W/(m*K)
Thermal conductivity of thawed ground	K_t	W/(m*K)
Volumetric water content	W_{vol}	Fraction of 1
Volumetric heat capacity of snow cover	C_{sn}	J/m^{3}K
Volumetric heat capacity of ground skeleton	C_{sk}	J/m^{3}K
Volumetric heat capacity of thawed ground	C_t	J/m^{3}K
Volumetric heat capacity of frozen ground	C_f	J/m^{3}K

Table 2 Output variables.

Output variables	Notation
Correction to T_a accounting for snow cover effect, °C	ΔT_{sn}
Correction to A_a accounting for snow cover effect, °C	ΔA_{sn}
Correction to T_a accounting for vegetation cover, °C	ΔT_v
Correction to A_a accounting for vegetation cover, °C	ΔA_v
Seasonal range of temperature variations at the ground surface, °C	A_{gs}
Mean annual temperatures at the ground surface, °C	T_{gs}
Thermal offset, °C	ΔT_k
MAGT, °C	T_{ps}
ALT, m	X

Evaluation of snow cover influence.

Snow cover plays an important role in heat exchange processes between the surface of the ground and the atmosphere. Snow cover influence is complex, working as an insulator for the ground throughout the winter, effectively increasing the MAGT, but when snow remains on the ground after air temperatures rise above freezing, the seasonal thawing can be delayed.

The warming effect of snow cover has been calculated using approximate formulas derived by Romanovsky (1987) and Lachenbruch (1959), which incorporate ground properties, vegetation cover, and their respective effect on heat turnovers through the snow. Heat turnovers are defined as the quantity of incident heat (during the heating period), or out going heat (during the cooling period) throughout the media over a given time interval (usually half year increments). So that the heat transport is

$$Q = \int_{t_1}^{t_2} q(t)dt$$

where t_1 and t_2 are the times when the regime changes from heating to cooling periods, or cooling to heating periods, and $q(t)$ is heat flux through the ground surface as a function of time.

The total thermal effect of snow cover on the seasonal amplitude of air temperatures ΔA_{sn} and mean annual air temperatures ΔT_{sn} is calculated

Copyright © 2003 John Wiley & Sons, Ltd.

as follows:

$$\Delta A_{sn} = \Delta A \frac{\tau_1}{\tau} \text{ and } \Delta T_{sn} = \frac{2}{\pi} \Delta A_{sn} \quad (1\text{–}2)$$

where τ is one year period, τ_1—is the duration of winter period and

$$\Delta A = A_a \left(1 - \frac{1+\mu}{\sqrt{s}} \right) \quad (3)$$

Where s is the mean thermal effect of snow cover, and is computed by:

$$s = e^{2H_{sn}\sqrt{\frac{\pi C_{sn}}{\tau K_{sn}}}} + 2\mu \cos\left(2H_{sn}\sqrt{\frac{\pi C_{sn}}{\tau K_{sn}}} \right) + \mu^2 e^{-2H_{sn}\sqrt{\frac{\pi C_{sn}}{\tau K_{sn}}}} \quad (4)$$

μ is a dimensionless parameter that characterizes the contrast in the thermal properties between snow cover and the underlying material (such as vegetation or different types of soils), and reflects the influence of the underlying material on the insulating effect of snow cover. H_{sn} is the winter-averaged snow cover thickness, C_{sn} is the average snow heat capacity, and K_{sn} is the average snow thermal conductivity. μ can range from -1 to $+1$ and is defined as:

$$\mu = \frac{\sqrt{K_{sn}C_{sn}} - \sqrt{K_f C_{ef}}}{\sqrt{K_{sn}C_{sn}} + \sqrt{K_f C_{ef}}} \quad (5)$$

where K_f is the frozen soil thermal conductivity and

$$C_{ef} = C_f \frac{\alpha - \beta}{(\alpha - \beta) - \ln \dfrac{\alpha + 1}{\beta + 1}} \quad (6)$$

where C_f is the frozen soil heat capacity. The parameter C_{ef} is the effective heat capacity of the substrate below snow cover. C_{ef} was derived taking into account heat turnover. The two dimensionless variables α and β are analogous to the Stefan number (which is the ratio of sensible and latent heats) in the Neumann equation (Zarling, 1987)

$$\alpha = \frac{2A_a C_f}{L} \quad (7)$$

$$\beta = \frac{2|T_a|C_f}{L} \quad (8)$$

where L is the volumetric latent heat of the water fusion in the ground. The result is that the mean annual temperature T_{vg} and the seasonal amplitude of temperatures A_{vg} on top of the vegetation cover are:

$$T_{vg} = T_a + \Delta T_{sn} \text{ and } A_{vg} = A_a - \Delta A_{sn}$$

The thermal effects of surface vegetation cover.

In our studies, only conductive heat transfer through the surface vegetation (lichens, moss, and grasses) was considered, even though this mechanism is a small part of the vegetation–ground interaction. The rate of heat turnover between the ground and atmosphere has been shown to have a strong dependence on vegetation cover. In summer, surface vegetation prevents solar radiation from penetrating into the ground and warming it. In wintertime, surface vegetation acts as an insulator and keeps heat in the ground.

For the purposes of the GIPL model, we assumed that the thermal conductivity of moss is 0.2 W/(m*K) (Kudryavtsev *et al.*, 1974) and for grass it is 0.3–0.5 W/(m*K). Heat capacities of moss and grass are about 2500–3000 kJ/m^3. The vegetation effect on the ground thermal regime was calculated using an algorithm suggested by Yershov (1998):

$$\tau_1 = \tau \cdot \left(0.5 - \frac{1}{\pi} \arcsin \frac{T_a}{A_a} \right), \tau_2 = \tau - \tau_1$$

where τ_1 and τ_2 are the winter cooling and summer warming periods respectively. The vegetation cover thermal effect for winter ΔA_1, and for summer ΔA_2 are:

$$\Delta A_1 = (A_{vg} - T_{vg}) \cdot \left(1 - e^{-H_{vg}\sqrt{\frac{\pi}{D_{vf}2\tau_1}}} \right) \quad (9)$$

$$\Delta A_2 = (A_a - T_a) \cdot \left(1 - e^{-H_{vg}\sqrt{\frac{\pi}{D_{vt}2\tau_2}}} \right) \quad (10)$$

Average thermal effect for seasonal amplitude of temperature variations ΔA_v and for mean annual temperature ΔT_v are calculated from:

$$\Delta A_v = \frac{\Delta A_1 \tau_1 + \Delta A_2 \tau_2}{\tau}$$

$$\Delta T_v = \frac{\Delta A_1 \tau_1 - \Delta A_2 \tau_2}{\tau} \frac{2}{\pi} \quad (11\text{–}12)$$

Copyright © 2003 John Wiley & Sons, Ltd.

From this result we can estimate the temperature on the surface of the ground T_{gs} and the seasonal amplitude of temperature variations at the ground surface A_{gs} as:

$$T_{gs} = T_{vg} + \Delta T_v \quad A_{gs} = A_{vg} - \Delta A_v \qquad (13\text{–}14)$$

Calculating the thermal offset and MAGT at the bottom of the active layer.

The seasonal freezing and thawing cycles cause changes in the thermal properties of soils within the active layer. Typically, this will lead to a decrease in MAGTs with depth. The thermal offset is defined as the difference between the mean annual temperature on the surface of the ground and the MAGT at the bottom of the active layer (Kudryavtsev *et al*., 1974; Goodrich, 1978; Burn and Smith, 1988). The thermal offset depends on soil moisture content and thermal properties, and has the most pronounced effect within a peat layer.

The analytical equation to estimate the thermal offset ΔT_k was given by Kudryavtsev (1981) (no derivation was published), and was formally derived by Romanovsky (Romanovsky and Osterkamp, 1995). The equation for thermal offset gives:

$$\Delta T_k = I_t(K_t/K_f - 1)/\tau \quad \text{for} \quad K_t I_t \le K_f I_f \qquad (15)$$

and

$$\Delta T_k = I_f(1 - K_f/K_t)/\tau \quad \text{for} \quad K_t I_t > K_f I_f \qquad (16)$$

where I_t and I_f are thawing and freezing indices at the ground surface. The freezing index is the absolute value of the sum of all negative mean daily ground surface temperatures (below 0 °C) during the calendar year. Equation 15 is for a seasonally thawed active layer that has permafrost underneath, and equation 16 is for a seasonally frozen soil layer that is on top of unfrozen ground. Seasonal temperature variation at the surface of the ground can be expressed by the harmonic function:

$$T(t) = T_{gs} + A_{gs} \sin\left(\frac{2\pi}{\tau} t\right)$$

and T_{ps} can be estimated by the formula:

$$T_{ps} = \frac{0.5T_{gs}(K_f + K_t) + A_{gs}\dfrac{K_t - K_f}{\pi} \times \left[\dfrac{T_{gs}}{A_{gs}} \arcsin \dfrac{T_{gs}}{A_{gs}} + \sqrt{1 - \dfrac{T_{gs}^2}{A_{gs}^2}}\right]}{K^*} \qquad (17)$$

where

$$K^* = \begin{cases} K_f, \text{ if numerator} < 0 \\ K_t, \text{ if numerator} > 0 \end{cases}$$

The Kudryavtsev's approach in calculating MAGT is the consecutive layer-by-layer introduction of thermal effects of snow, ground surface vegetation, and the soils within the active layer on mean annual temperatures and seasonal amplitudes at each considered level (snow surface, vegetation surface, ground and permafrost surfaces). However, this scheme is not totally additive because estimation of the impact of each new layer already includes the thermal effects of all layers above it. Moreover, in the mKA, the thermal effect of snow reflects the thermal properties and temperature field dynamics in the subsurface layers through the heat turnover estimation (see the *Evaluation of the snow cover influence*). As a result, the mKA takes into account some negative and positive feedbacks between designated layers in the 'atmosphere-permafrost' system.

Calculating ALT.

Calculation of ALT using Kudryavtsev's formula is the final step in the model (Romanovsky and Osterkamp, 1997). The formula was derived for homogeneous ground, but in actuality, even if soil properties are the same throughout the active layer, the moisture content or mode of heat flow may vary significantly. This can make the active layer inhomogeneous with regard to its thermal properties. Also, the model does not take into account unfrozen water, which can exist in the frozen active layer even at relatively cold temperatures (−5 °C or colder), and has a significant effect on the grounds thermal properties (Williams, 1964; Williams and Smith, 1989). The assumption of a periodically steady-state temperature regime seems to be a good approximation when applied to the annual temperature cycle, which varies from year to year (Romanovsky and Osterkamp, 1997). Considering the advantages along with the shortcomings, the formula appears to give a good representation of the coupling between permafrost and the atmosphere.

Evaluating the Performance of the mKA

Two methods have been applied to determine the accuracy of the mKA approach for ALT and MAGT calculations. First, the results of the mKA approach were compared with numerical model outcomes. Second, the analytical results were compared with measured ALT and MAGTs taken from sites along the east Siberian and Alaskan transects.

Copyright © 2003 John Wiley & Sons, Ltd.

Comparison of mKA approach to a numerical model.

The numerical model chosen to compare to the mKA results was developed by G. S. Tipenko of the Moscow State University, presently at the Geophysical Institute, University of Alaska Fairbanks. This model solves the one-dimensional heat conduction equation in a non-homogeneous media, containing unfrozen water. The model was successfully used for the ground temperature regime reconstruction at the Barrow Permafrost Observatory during the period 1924–2001 (Romanovsky *et al*., 2002). The numerical model accounts for snow cover by treating it as part of the upper boundary conditions together with air temperatures. This approach was applied to Barrow and Fairbanks in the Alaskan transect, and to Tiksi and Yakutsk in the east Siberian transect. For each location, five different forecasts were done for the period 2000–2099. Each of the forecasts used mean monthly air temperatures and snow thickness output from the respective GCMs. The five ACIA-designated GCMs were provided by the Canadian Center for Climate Modeling and Analysis (CCC model), the National Center for Atmospheric Research/Climate System Model (CSM model), the Geophysical Fluid Dynamics Laboratory (GFDL model), the Hadley Climate Center (HadCM3 model), and the Max Plank Institute for Meteorology (ECHAM model).

The thermophysical properties of the ground that were used for the numerical model have been taken from previous studies (Romanovsky and Osterkamp, 1995; Romanovsky and Osterkamp, 2000; Romanovsky *et al*., 2001). These thermophysical properties have been averaged for the purposes of applying them to Kudryavtsev's formula. These averages take into account the thickness of each layer in the ground. The results are presented in Figures 2 through 5.

To evaluate how the mKA corresponds to the numerical model, a linear regression technique has been applied (Table 3). The slope of the least squares fit ranges from 0.6 to 1.35, and the slope of ALT varies from 0.4 to 1.1. This shows good agreement between the mKA and numerical models. The correlation coefficient and the P-value (probability that the correlation coefficient is zero) have also been calculated. The results show a strong correlation for ALT and MAGTs between mKA and the numerical model, with correlation coefficients between 0.7–0.9 and a P-value close to 0.

The mKA and the numerical model show similar variations in ALT calculations (Figures 2 and 3). For all the GCM scenarios that have been analysed

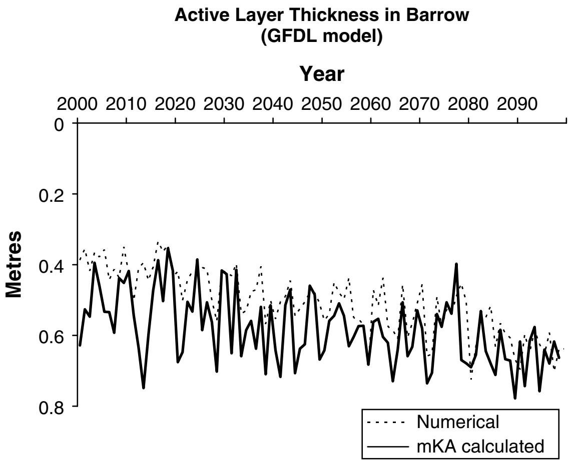

Figure 2 ALT calculated using numerical model and mKA for Barrow.

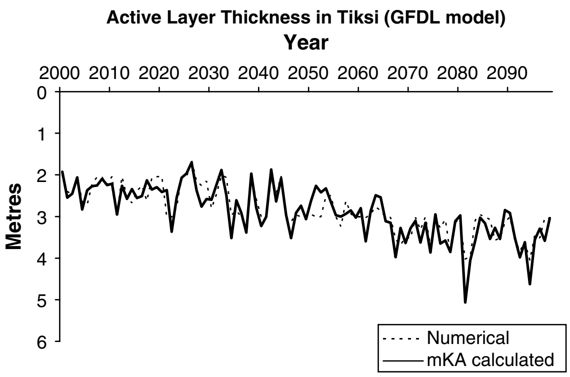

Figure 3 ALT calculated using numerical model and mKA for Tiksi.

(excluding CSM), the differences in the calculated ALT on the 100-year interval did not exceed 0.3 m. Using CSM results, the difference between the two models was 0.48 m. The numerical model accounts for unfrozen water content, which results in phase transitions at temperatures less than 0 °C. This results in the mKA giving deeper active layer values for most scenarios.

Also, for most scenarios, the mKA approach gives slightly warmer temperatures than the numerical model for the years 2000–2050, and gives colder temperatures for 2050–2100 (Figure 4). Additional work will be needed to determine the nature of these biases. The steady-state periodical regime on the surface, which is one of the assumptions used in mKA, is one possible explanation for this. For all

Copyright © 2003 John Wiley & Sons, Ltd.

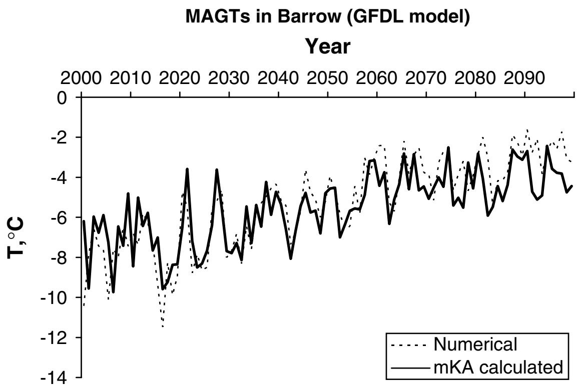

Figure 4 MAGTs calculated using numerical model and mKA for Barrow.

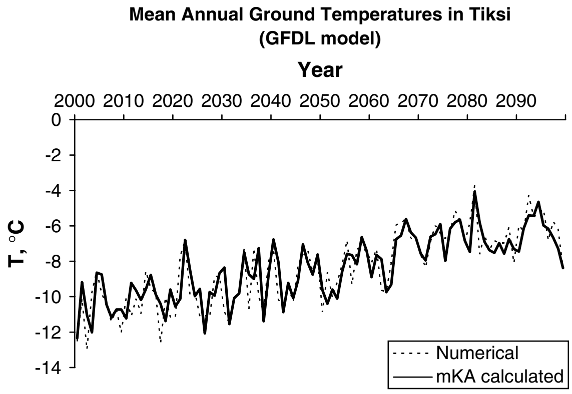

Figure 5 MAGTs calculated using numerical model and mKA for Tiksi.

scenarios, the difference between averaged over all years MAGTs given in the mKA and the numerical model is within 0.3 °C.

Comparison with measured MAGT.

The next step was to compare the mKA values with measured MAGTs and ALT from data sites along the transects. There is a lack of long-term data (on the scale of 20–40 years) for the Alaskan transect, and an overall lack of ALT data from the east Siberian transect. Because of this, only seven points were chosen from each transect to evaluate error in the MAGT and ALT calculations.

Monthly air temperatures and snow cover thickness were recorded for all points chosen, but thermophysical properties of the soils (Table 4) were not available for the individual sites. To account for the lack of soil properties, we used the *Geocryological Map of the USSR* (1997) for the east Siberian transect, and properties of the Alaskan transect were taken from Brown and Kreig (1983).

Table 3 Statistical analysis of Kudryavtsev's model correspondence with numerical model.

	MAGT				ALT			
Station, GCM	Intercept	Slope	Correlation	P-value	Intercept	Slope	Correlation	P-value
Barrow, CCC	−1.54	0.63	0.87	<0.0001	−0.20	0.94	0.85	<0.0001
Barrow, CSM	−1.90	0.79	0.71	<0.0001	0.13	0.72	0.32	0.00
Barrow, ECHAM	−1.81	0.78	0.92	<0.0001	0.22	0.91	0.82	<0.0001
Barrow, GFDL	−2.20	0.63	0.82	<0.0001	0.25	0.66	0.63	<0.0001
Barrow, HAD3	−1.77	0.67	0.87	<0.0001	0.23	0.82	0.74	<0.0001
Fairbanks, CCC	−0.13	1.35	0.85	<0.0001	−0.20	0.94	0.85	<0.0001
Fairbanks, CSM	−0.03	1.35	0.58	<0.0001	—	—	—	—
Fairbanks, ECHAM	−0.22	1.16	0.87	<0.0001	—	—	—	—
Fairbanks, GFDL	−0.22	1.16	0.84	<0.0001	—	—	—	—
Fairbanks, HAD3	−0.24	1.31	0.79	<0.0001	—	—	—	—
Tiksi, CCC	−1.17	0.83	0.94	<0.0001	−0.55	1.11	0.86	<0.0001
Tiksi, CSM	−1.19	0.91	0.88	<0.0001	−0.27	0.61	0.74	<0.0001
Tiksi, ECHAM	−1.24	0.83	0.94	<0.0001	−0.41	1.04	0.92	<0.0001
Tiksi, GFDL	−1.87	0.77	0.87	<0.0001	0.03	1.00	0.88	<0.0001
Tiksi, HAD3	−1.65	0.85	0.90	<0.0001	0.31	0.82	0.75	<0.0001
Yakutsk, CCC	−0.48	0.84	0.90	<0.0001	0.56	0.55	0.81	<0.0001
Yakutsk, CSM	−0.87	0.88	0.71	<0.0001	0.41	0.39	0.41	<0.0001
Yakutsk, ECHAM	−0.15	0.96	0.87	<0.0001	0.56	0.54	0.78	<0.0001
Yakutsk, GFDL	−1.02	0.76	0.86	<0.0001	0.30	0.67	0.79	<0.0001
Yakutsk, HAD3	−0.74	0.74	0.86	<0.0001	0.50	0.59	0.79	<0.0001

Copyright © 2003 John Wiley & Sons, Ltd.

Table 4 Thermophysical properties for the sites within east Siberian transect.

Station	Volumetric water content	Thermal conductivity of frozen soils W/(m*K)	Thermal conductivity of thawed soils W/(m*K)
Amga	0.20	2.36	1.91
Isit	0.65	1.37	0.96
Namtsy	0.20	1.39	0.88
Krest-Khaldzai	0.04	1.39	1.38
SanYakhtat	0.20	1.95	1.43
Verkhoyansk	0.20	2.36	1.35
Nyurba	0.20	2.22	1.71

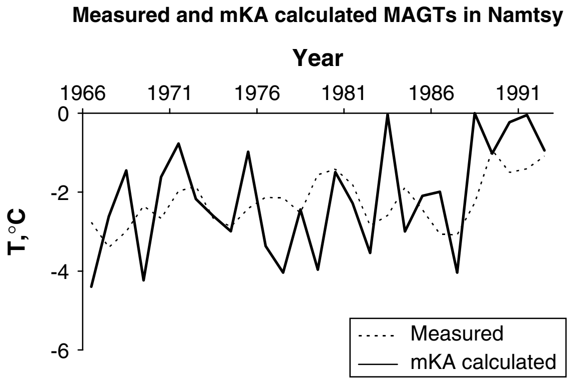

Figure 7 Measured and calculated MAGTs for Namtsy.

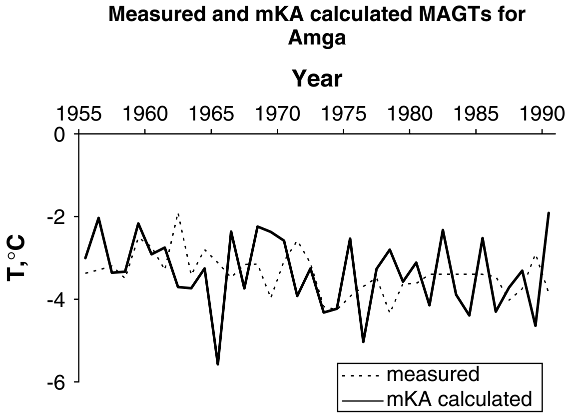

Figure 6 Measured and calculated MAGTs for Amga.

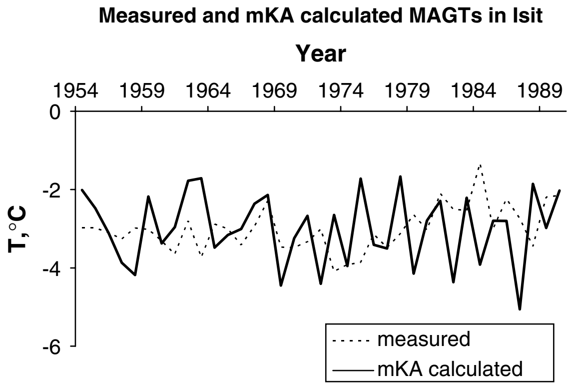

Figure 8 Measured and calculated MAGTs for Isit.

The difference between the measured and calculated values of the MAGT can reach 1.5–2 °C for certain years. However, when averaged over the entire time interval, this difference does not exceed 0.3 °C (Table 5). The interval is different for each meteorological station, and ranges from 1970–1990 at Verkhoyansk, to 1935–1990 at Krest-Khaldzai. Generally, the mKA gives slightly colder temperatures for points within the east Siberian transect (Table 5). The calculated MAGTs have a greater magnitude for interannual fluctuations than the measured values yield (Figures 6 through 8).

Table 5 Comparison of calculated and measured MAGTs for east Siberian transect.

Station	Years	Measured MAGT, °C	Calculated MAGT, °C	Difference, °C
Amga	1955–1990	−3.38	−3.34	−0.04
Isit	1954–1990	−3.01	−2.99	−0.02
Namtsy	1966–1992	−2.25	−2.16	−0.09
Krest-Khaldzai	1970–1991	−3.80	−3.78	−0.02
SanYakhtat	1963–1988	−0.46	−0.31	−0.15
Verkhoyansk	1935–1990	−7.67	−7.43	−0.24
Nyurba	1956–1990	−1.01	−0.75	−0.26

Copyright © 2003 John Wiley & Sons, Ltd.

Table 6 Comparison of calculated and measured ALT for Alaskan transect.

Station	Years	Measured ALT, m	Calculated ALT, m	Relative error, %
Franklin Bluffs	1990–2000	0.65	0.59	9
Dead Horse	1990–2001	0.60	0.46	23
Happy Valley	1993–2000	0.44	0.59	32
Bonanza Creek	1990–2000	0.50	0.59	17
Barrow	1991–2000	0.33	0.26	20
Pearl Creek	1990–2000	0.62	0.67	8
Toolik Lake	1990–2001	0.40	0.33	16
Ivotuk 1	1999–2001	0.59	0.43	27

The measured values of ALT were supplied by the Circumpolar Active Layer Monitoring (CALM) network (www.geography.uc.edu/~kenhinke/CALM). Analysis shows that the relative error of the averaged-over entire period of available data ALT calculations is lower than 32%. For about half of the points, the mKA gives a shallower ALT than was measured (Table 6). The primary source of error might be the uncertainty in setting snow and vegetation cover parameters which were not known. This error is of particular concern with regard to the thermal diffusivity of vegetation.

GIS Approach for Evaluating the Spatial Dynamics of ALT and MAGTs

GIS are widely used to store and analyse large volumes of data. They allow visualization of the spatial distribution of topographic features such as soil types, vegetation and climatic parameters, as well as the incorporation of modelling results. We have applied a GIS approach to evaluate the spatial dynamics of ALT and MAGTs along the two transects.

Each database that was used contains layers representing soils, vegetation cover, meteorological data, rivers, elevation, permafrost distribution, etc (Romanovsky *et al.*, 2001). Climate data, including mean annual air temperatures, the range of mean monthly air temperatures, and snow cover thickness and density from GCMs have been incorporated into these databases.

Once compiled, the datasets contain all the necessary parameters for calculation of ALT and MAGTs for the period from 1900–2100. Seasonal air temperature range and average winter snow thickness and density were supplied by the GCMs; but there were not enough data available on vegetation cover changes and soil properties for the same time period. When calculating past and present ALT and MAGTs, we assumed that these uncertainties were relatively small and did not effect the permafrost dynamics of interest. The calculations for both transects were performed using a uniform spatial grid with a resolution of $0.5 \times 0.5°$ latitude/longitude. The spatial grids for the Alaskan and east Siberian transects contain 517 and 1000 grid cells respectively. Figure 9 shows an example of the results obtained with GIPL using the HadCM2 GCM that was developed in the Hadley Climate Center. Results using other GCM outputs can be obtained through the ACIA project.

The procedure used to calculate the ALT and MAGTs for a given year is demonstrated by the block diagram shown in Figure 10. One external script and two internal scripts have been written to create a user-friendly interface for the evaluation of MAGT. The first internal script obtains information from the user for which year(s) the calculations should be performed. These input parameters are sent to the external script. The external script uses mKA to calculate ALT and MAGT for each point on the grid.

The first internal script activates the second internal script, which takes the results from the new file, which was created by the external script. The script then performs the interpolation between the points using an inverse distance weighted (IDW) interpolator. Two gridded output files are created; one for ALT and another for MAGTs. The second internal script assigns a prescribed colour scale for visualization of each of the grid cells. Another important function of the second internal script is the extraction of the area where the MAGTs are positive (above 0 °C). This is important because if an area has a positive MAGT, permafrost degradation has begun.

Through a combination of Kudryavtsev's approach and the GIS method of data storing and processing, the quasi-two-dimensional, quasi-transitional, spatially distributed, analytical model for ALT and MAGT calculations has been developed. This model has been called the GIPL model, and can be referred to as an interactive GIS because input parameters can be easily changed and yield new results instantly.

The Overall Performance of the GIPL Model

A method of statistical analysis has been applied to determine the overall performance of the model. Soil temperatures that have been measured daily and stored as monthly means at 52 different weather stations along the transect were used for the analysis. MAGTs at the bottom of the active layer were calculated for each station. These data are available from the Joint Office of Science Support

Copyright © 2003 John Wiley & Sons, Ltd.

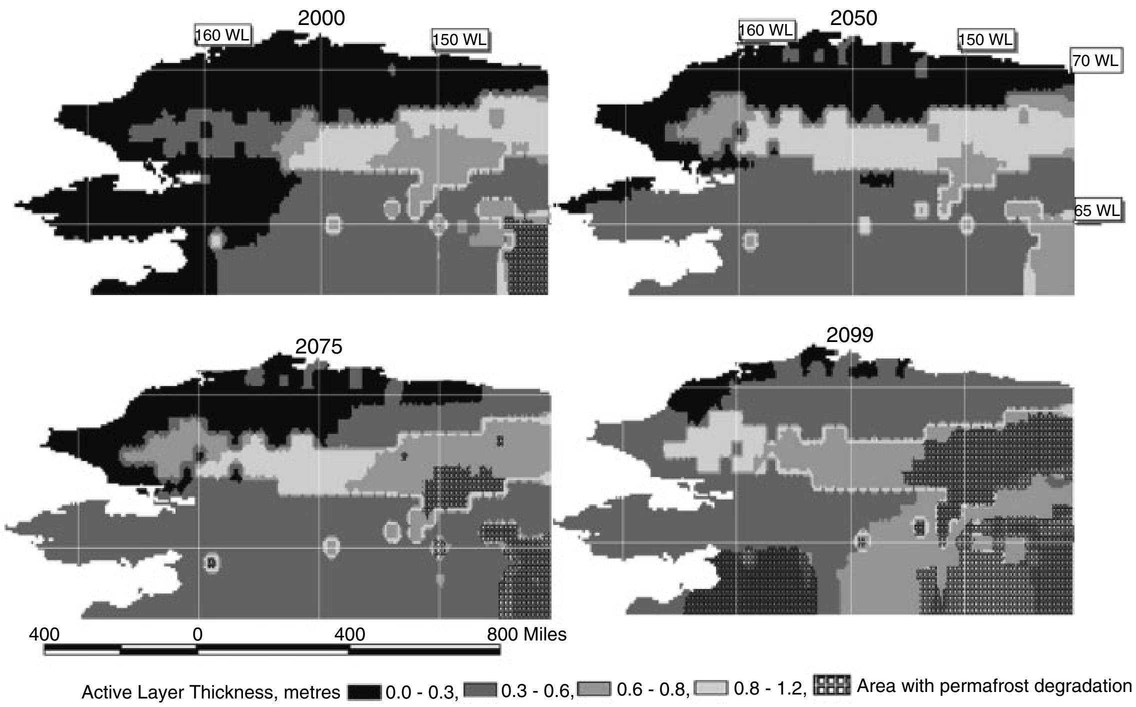

Figure 9 ALT for the east Siberian transect (Had CM2 GCM).

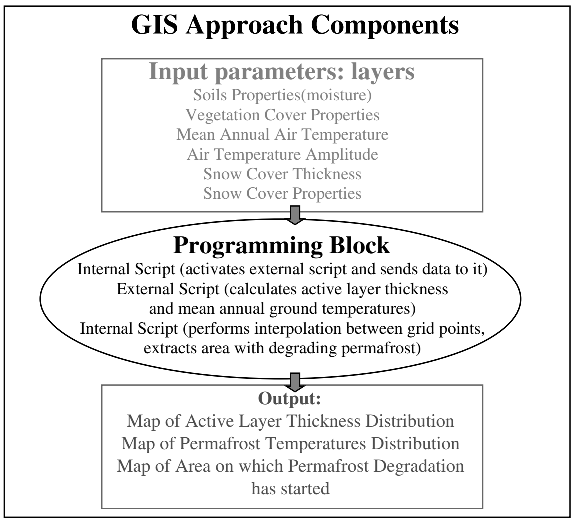

Figure 10 Block diagram of GIS approach.

(JOSS) and can be obtained at www.joss.ucar.edu; the dataset name is 'ATLAS: 1899–1994, and contains the East-Siberian Transect—air and ground temperatures and snow depth (Romanovsky).'

Originally, this dataset was compiled and digitized by our collaborators on this project from the Permafrost Institute in Yakutsk (group leader V. T. Balobaev) and at the Institute of Physico-chemical and Biological Problems in Soil Science, Russian Academy of Sciences (group leader D. A. Gilichinsky) using published monthly meteorological regional reports (Klimatologicheskii sravochnik SSSR, 1961–1992). From those sites only 32 points were chosen on the basis of data quality and measurement consistency. Ground temperature measurements taken at a depth of 1.6 m during a 24-year period from 1966–1989 were used for comparison with the calculated MAGTs. Even though it would be better to compare with temperatures measured deeper at 2.4 or 3.2 m, we chose the depth of 1.6 m because of the higher consistency of measurements and availability. At one third of the meteorological stations ground temperatures below 1.6 m were not measured. This particular depth matches very well the depth of the permafrost table at the most sites used in this research. Only eight out of 32 sites show the active layer deeper than 1.6 m and at only three of them was the ALT in excess of 2.4 m. Because the most significant changes in MAGTs due to the thermal offset take place within the upper third of the active layer (Burn and

Copyright © 2003 John Wiley & Sons, Ltd.

Smith, 1988; Romanovsky and Osterkamp, 1995), the measured mean annual temperatures at 1.6 m can represent MAGTs very well even for sites with a deeper active layer. The long-term difference between mean annual temperatures at 1.6 m and 3.2 m will typically not exceed 0.3 °C.

Air temperature measurements are available for all data sites, and the snow cover thickness is available for eight of them. We have extrapolated snow thickness along the entire transect. The MAGTs were calculated using the GIPL model for each of the 32 sites for every year from the interval of 1966 to 1989, and these values were compared with the measured values. Two digital maps have been created using IDW interpolation between the points (Figure 11). It should be noted that most of the sites are in the central and southern parts of the transect. This is probably why calculated MAGTs for the higher latitudes do not correlate well with the measured temperatures.

Differences between the measured and calculated values for MAGTs over a 24-year period varied from 0.2 to 0.6 °C (Figure 11). In the southern regions of the transects, the GIPL model gives colder MAGTs while the model gives warmer than measured temperatures in the western part of the transect, with differences varying from 0.2–0.4 °C. When averaged over the entire 24-year period of calculations, the difference between the measured and calculated values did not exceed 0.6 °C and is around 0.3 °C for most base points.

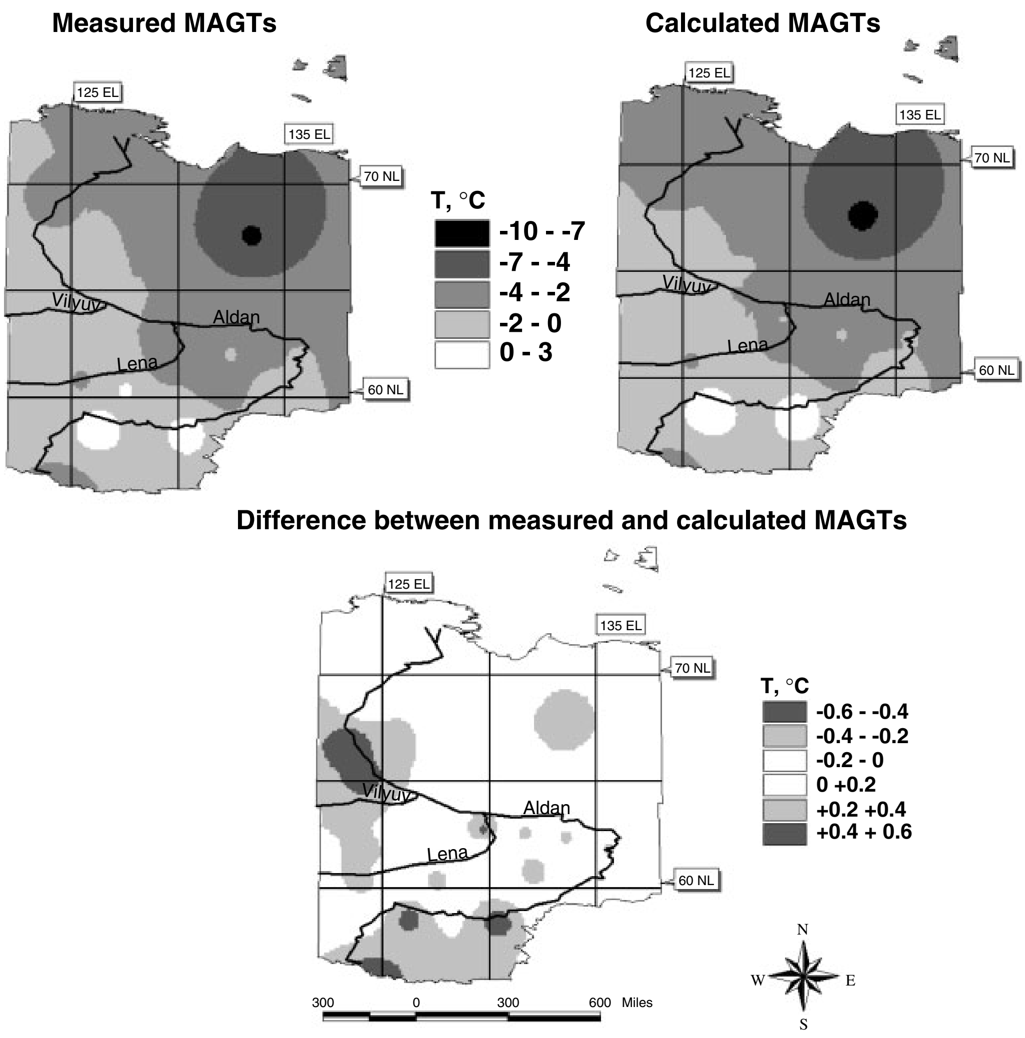

Figure 11 Calculated and measured MAGTs for east Siberian transect.

Copyright © 2003 John Wiley & Sons, Ltd.

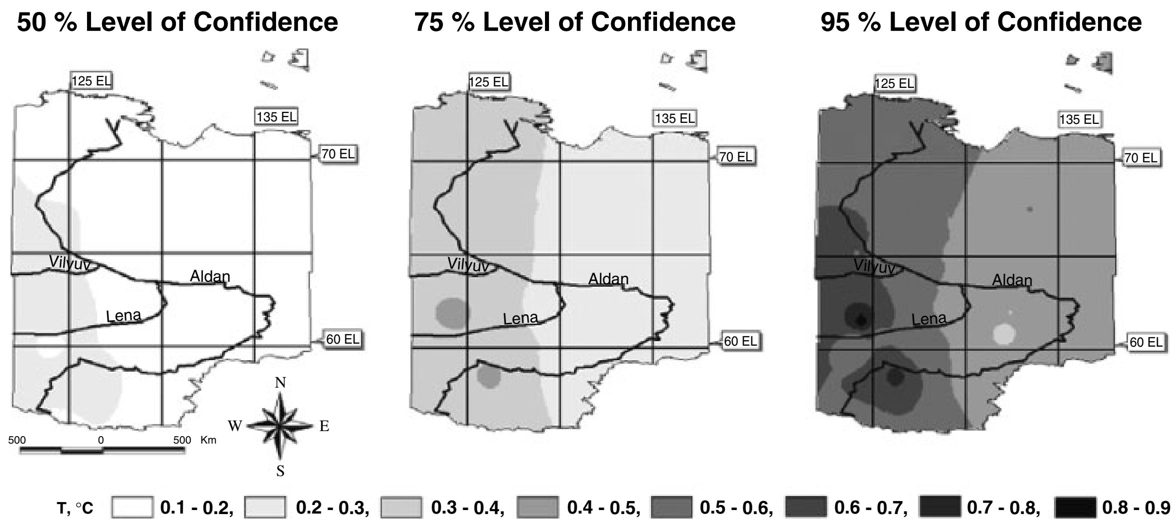

Figure 12 Ranges of variation of MAGTs with certain levels of confidence.

In order to determine the uncertainty associated with the MAGT calculations, a confidence analysis was performed which provides the confidence interval for a population mean (in our case, averaged MAGT over a 24-year interval). The analysis was performed for 50%, 75%, and 95% levels of confidence (Figure 12). The interpretation of the results must include the confidence interval as it shows the range on either side of the MAGT averaged over the years 1966–1989.

The results of the confidence analysis show that with a 50% confidence, the calculated MAGT will not differ from measured temperatures by more than 0.1–0.2 °C for the eastern, central, northern and southeastern parts of the transect. In the western part of the transect, the measured and predicted MAGTs do not differ by more than 0.2–0.3 °C. For a 75% confidence level, we can expect that differences in calculated and measured temperatures range from 0.2–0.3 °C for the eastern part of the transect (to the east from 130° EL) and in the range of 0.3–0.4 °C for the western part. If confidence level is 95%, the difference between calculated and measured temperatures can reach up to 0.4–0.5 °C for the eastern part of the transect, and 0.6–0.8 °C for the western part.

The confidence analysis has shown that in the western part of the transect (roughly the area between 120° and 130° EL) a greater level of uncertainty and wider differences between calculated and measured MAGTs might be expected. For the eastern part of the transect, the range of differences between calculated MAGTs and measured values is not as large as in the western part of the transect. Additional investigations and data on snow and vegetation cover properties are required to explain the results of the confidence analysis more thoroughly. With the data that are currently available, the variance in the uncertainty between the eastern and western parts of the transect can be explained by deeper snow cover (0.4–0.8 m) and greater interannual variations in snow cover thickness in the western part of the transect. A level of confidence of 75% is considered to be appropriate for engineering and scientific purposes. We assume that calculated mean annual temperatures are equal to measured MAGTs with a 0.2–0.4 °C uncertainty. Unfortunately, it was not possible to perform the same analysis for the ALT for the east Siberian transect due to the lack of ALT measurements. Long-term data on the ALT is available only for 10 points from the Alaskan transect and measurements were not taken consistently, so we could not perform the same statistical analysis. Instead, calculated and measured ALTs were compared (Table 6). From this analysis it is clear that the relative error of ALT calculations does not exceed 33% with most typical relative errors between 15 and 25%. These relative errors can be assumed to be acceptable for the regional scale analysis especially if very high natural variability in ALT is taken into account. Our data from the North Slope of Alaska show that natural variability in ALT within the 100 × 100 m sampling grids is typically in the range of 15–35%.

Copyright © 2003 John Wiley & Sons, Ltd.

CONCLUSIONS

A quasi-two-dimensional, quasi-transitional, spatially distributed, analytical model for ALT and MAGT calculations has been developed (GIPL model). GIPL can be referred to as an interactive GIS because input parameters can be easily changed and yield new results instantly. The mKA was chosen for ALT and MAGT calculations in this model. When applied to long-term (decadal and longer time scale) averages, this approach shows an accuracy of $\pm 0.2-0.4\,^{\circ}$C for the MAGTs and $\pm 0.1-0.3$ m for the ALT calculations. The relative errors do not exceed 32% for ALT calculations, but typically they are between 10 and 25%.

The differences in 0.2–0.4 °C between calculated and measured MAGTs were obtained for the long-term multi-year average estimations, not for specific years (when these differences could be as large as 1.5 to 2 °C). This inadequacy of measured and calculated parameters on a year-by-year basis can be explained by errors in snow thickness and density estimations and approximations of thermophysical parameters of soils, as well as the assumption of a periodical quasi-steady-state temperature regime. However, for permafrost stability assessment the long-term averages are the most important.

The comparison of Kudryavtsev's approach with a numerical model shows good correlation. Small errors in estimation of permafrost parameters, attributed mostly to limitations in Kudryavtsev's approach, result from not taking into account unfrozen water dynamics. The results obtained from this comparison show that a more economical (in terms of computational time) analytical approach could be successfully used instead of a full-scale numerical model in the regional and global scale analysis of permafrost spatial and temporal dynamics.

The spatial statistical evaluation of the GIPL model performance using data from 32 sites within the east Siberian transect showed that with 75% probability the confidence interval averaged over 24 years MAGTs can deviate from the measured temperatures by not more than $\pm 0.3\,^{\circ}$C for the eastern part of the transect (to the east from 130° EL) and by not more than $\pm 0.4\,^{\circ}$C for the western part.

The analysis performed for two transects validated the use of Kudryavtsev's approach and our GIPL model for calculating ALT and MAGTs. This analysis shows that GIPL can be successfully used in regional assessments of permafrost stability and dynamics.

ACKNOWLEDGEMENTS

This research was funded by the Polar Earth Science Program and by ARCSS Program, Office of Polar Programs, National Science Foundation (OPP-9870635, OPP-9721347, OPP-9732126), and by the State of Alaska. The temperature data used in this study are available to other researchers through the JOSS project (http://www.joss.ucar.edu) and NSIDC (http://nsidc.org). We would like to thank Dr C. R. Burn and an anonymous reviewer for very helpful suggestions that were used to improve the manuscript.

REFERENCES

Anisimov OA, Nelson FE. 1997. Influence of climate change on continental permafrost in the northern hemisphere. *Meteorologiya i Gidrologiya* **5**: 71–80 (in Russian; English translation appears in *Russian Meteorology and Hydrology* 1997/5).

Anisimov O, Fitzharris B, Hagen JO, Jeffries R, Marchant H, Nelson FE, Prowse T, Vaughan DG. 2001. Polar Regions (Arctic and Antarctic). *Climate Change: Impacts, Adaptation, and Vulnerability, the Contribution of Working Group II of the Intergovernmental Panel on Climate Change, Third Assessment Review*. Cambridge University Press: Cambridge; 801–841.

Brown J, Kreig RA. 1983. Guidebook to permafrost and related features along the Elliot and Dalton highways, Fox to Prudhoe Bay, Alaska. *Proceedings of Fourth International Conference on Permafrost. 18–22 July 1983*, Alaska Division of Geological and Geophysical Surveys, Department of Natural Resources, State of Alaska, Fairbanks, Alaska, 230 pp.

Burn CR, Smith CAS. 1988. Observations of the 'thermal offset' in near-surface MAGTs at several sites near Mayo, Yukon Territory, Canada. *Arctic* **41**(2): 99–104.

Feldman GM, Tetelbaum AS, Shender NI, Gavriliev RI. 1988. *The guidebook for temperature regime forecast in Yakutia* (in Russian), Yakutsk, Permafrost Institute Press, 240 pp.

Friend AD, Stevens AK, Knox RG, Cannell MGR. 1997. A process-based, terrestrial biosphere model of ecosystem dynamics (Hybrid v3.0). *Ecological Modeling* **95**: 249–287.

Geocryological Map of Russia and Neighbouring Republics. Scale 1 : 2,500,000. Moscow State University, Russian Ministry of Geology (English language edition) 1999. Geotechnical Science Laboratories, Department of Geography, Carleton University, Ottawa, Canada.

Goodrich LE. 1978. Some results of numerical study of ground thermal regime. *Proceedings of the Third International Conference on Permafrost*. National Research Council of Canada, Ottawa, vol. 1, 29–34.

Hinzman LD, Goering DJ, Li S, Kinney TC. 1997. Numeric simulation of thermokarst formation during

Copyright © 2003 John Wiley & Sons, Ltd.

disturbance. *Disturbance and Recovery in Arctic Lands: an Ecological Perspective*, Crawford RMM (ed.). Kluwer Academic Publishers: Dordrecht, The Netherlands; V. 25, 191–211.

Kane DL, Hinzman LD, Zarling JP. 1991. Thermal response of the active layer in a permafrost environment to climatic warming. *Cold Regions Science and Technology* **19**(2): 111–122.

Kattenberg A, Giorgi F, Grassl H, Mechl GA, Mitchell JFB, Stouffer RJ, Tokioka T, Weaver AJ, Wigley TML. 1996. Climate Models-Projections of Future Climate. In *Climate Change 1995, The Science of Climate Change, Contribution of Working Group I to the Second Assessment of the Intergovernmental Panel on Climate Change (Ch. 6)*, Houghton JT, Meira Filho LG, Callander BA, Harris N, Kattenberg A, Maskell K (eds). Cambridge University Press: Cambridge, U.K., 289–357.

Klimatologicheskii spravochnik SSSR, 1961–1992. Vypusk 24, po Yakutskoi ASSR, severnoi chasti Khabarovskogo kraya, Magadanskoi oblasti i severnoi chasti Kamchatskoi oblasti. Meteorologicheskie ezhemesyachnie dannye za 1961–1992, chast' II, VII, *Temperatura pochvy, tumany, grozy, meteli i grad*, Gidrometeoizdat, Leningrad (In Russian).

Kudryavtsev VA (ed.). 1981. *Permafrost (short edition)* (in Russian), Moscow State University Press, 240 pp.

Kudryavtsev VA, Garagula LS, Kondrat'yeva KA, Melamed VG 1974. *Osnovy merzlotnogo prognoza* (in Russian). Moscow State University Press (431 pp.) [CRREL Translation: VA Kudryavtsev, LS Garagula, KA Kondratiyeva, VE Melamed. *Fundamentals of Frost Forecasting in Geological Engineering Investigations*, CRREL Draft Translation 606, 1977, 489 pp.].

Lachenbruch AH. 1959. *Periodic heat flow in a stratified medium with application to permafrost problems*. US Geological Survey Bulletin, 1083-A, 36 pp.

Nelson FE, Outcalt SI. 1987. A frost index number for spatial prediction of ground frost zones. *Arctic and Alpine Research* **19**: 279–288.

Osterkamp TE, Esch DC, Romanovsky VE. 1997. Infrastructure: effects of climatic warming on planning, construction and maintenance. In *Implications of Global Change in Alaska and the Bering Sea Region, Proceedings of the BESIS Workshop, June*, 3–6, 1997, Center for Global Change and Arctic System Research, UAF, Fairbanks, Alaska, 115–127.

Péwé TL. 1983. Alpine permafrost in the contiguous United States: A Review. *Arctic and Alpine Research* Vol 15, N2, 145–156.

Potter C, Wang S, Nikolov NT, McGuire AD, Liu J, King AW, Kimball JS, Grant RF, Frolking SE, Clein JS, Chen JM, Amthor JS. 2001. Comparison of boreal ecosystem model sensitivity to variability in climate and forest site parameters. *Journal of Geophysical Research—Atmospheres* **106**: 33 671–33 688.

Romanovsky VE. 1987. Approximate calculation of the insulation effect of the snow cover. In *Geokriologicheskie Issledovania* (in Russian), Moscow State University Press, vol. 23, 145–157.

Romanovsky VE, Osterkamp TE. 1995. Interannual variations of the thermal regime of the active layer and near-surface permafrost in Northern Alaska. *Permafrost and Periglacial Processes* **6**(4): 313–335.

Romanovsky VE, Osterkamp TE. 1997. Thawing of the active layer on the coastal plain of the Alaskan Arctic. *Permafrost and Periglacial Processes* **8**(1): 1–22.

Romanovsky VE, Osterkamp TE. 2000. Effects of unfrozen water on heat and mass transport processes in the active layer and permafrost. *Permafrost and Periglacial Processes* **11**: 219–239.

Romanovsky V, Smith S, Yoshikawa K, Brown J. 2002. Permafrost temperature records: Indicators of climate change. *EOS, Transactions, AGU* **83**: 589–594.

Romanovsky VE, Shender NI, Sazonova TS, Balobaev VT, Tipenko GS, Rusakov VG. 2001. Permafrost Temperatures in Alaska and East Siberia: Past, Present and Future. *Proceedings of the Second Russian Conference on Geocryology (Permafrost Science)*, Moscow State University Press, June 6–8, 301–314.

Shender NI, Romanovsky VE, Tetelbaum AS. 1999. A forecast of the natural variability of climate in Yakutsk and Fairbanks (in Russian). *Science and Education* **2**: 24–29.

Shiklomanov NI, Nelson FE. 1999. Analytic representation of the active layer thickness field, Kuparuk River Basin, Alaska. *Ecological Modelling* **123**: 105–125.

Smith SL, Burgess MM. 1999. Mapping the sensitivity of Canadian permafrost to climate warming. *Proc. IUGG 99 Symp. HS2*, IAHS Publications 256, 71–80.

Stendel M, Christensen JH. 2002. Impact of global warming on permafrost conditions in a coupled GCM. *Geophys. Res. Lett.* **29**(13): 10-1–10-4.

Tikhonov AN, Samarsky AA. 1966. *Uravneniya Matematicheskoi Fiziki (*Equations of Mathematical Physics*)*. Nauka: Moscow, 540 pp.

Williams PJ. 1964. Unfrozen water content of frozen soils and soil moisture suction. *Geotechnique* **14**(3): 231–246.

Williams PJ, Smith MW. 1989. *The Frozen Earth: Fundamentals of Geocryology*. Cambridge University Press, 306 pp.

Yershov ED. 1998. *General Geocryology*. Cambridge University Press, 580 pp.

Zarling JP. 1987. Approximate solutions to Neumann problem. *ASME invited paper, International Symposium on Cold Regions Heat Transfer, Edmonton, Alberta*, 47–54.

Zhang T, Heginbottom JA, Barry RE, Brown J. 2000. Further statistics on the distribution of permafrost and ground ice in the Northern Hemisphere. *Polar Geography* **24**: 126–131.

Copyright © 2003 John Wiley & Sons, Ltd.